Amphoterin-Induced Gene and Open Reading Frame 2 (AMIGO2) Interacts with CAPN2 and Promotes the Proliferation and Migration of Hypopharyngeal Cancer Cell

Wei Gu
Peking Union Medical College Hospital
Yanyan Niu
Peking Union Medical College Hospital
Hong Huo
Peking Union Medical College Hospital
Dahai Yang
Peking Union Medical College Hospital
Xiaofeng Jin
Peking Union Medical College Hospital
Jian Wang (wangjianent@126.com)
Peking Union Medical College Hospital

Research Article

Keywords: AMIGO2, CAPN2, Hypopharyngeal Neoplasms, Cell Proliferation, Cell Migration

Posted Date: April 18th, 2022

DOI: https://doi.org/10.21203/rs.3.rs-1508019/v1

Abstract

Background: Amphoterin-induced gene and open reading frame 2 (AMIGO2) has been reported to play a detrimental role in multiple cancer types. However, the precise role of AMIGO2 in hypopharyngeal squamous cell carcinoma (HPSCC) remains elusive.

Methods: Bioinformatic analysis was employed to identify the differential expression and prognostic value of AMIGO2 in the head and neck cancer. Proliferation, apoptosis, and migration assays were then conducted after short hairpin RNA-mediated knockdown of AMIGO2 in FaDu cell line and in xenograft mouse model. Co-immunoprecipitation and mass spectrometry analysis were performed to determine the protein interaction between AMIGO2 and *CAPN2*. Rescue experiments with respect to the overexpression of *CAPN2* were also performed. RNA sequencing after AMIGO2 knockdown with and without *CAPN2* overexpression were conducted, followed by pathway enrichment analysis.

Results: AMIGO2 expression was up-regulated in head and neck cancer and correlated with a poor prognosis. Functionally, HPSCC cell proliferation and migration were significantly inhibited *in vivo* and *in vitro* upon AMIGO2 knockdown. AMIGO2 binds to *CAPN2* in cell context, and overexpression of *CAPN2* could effectively reverse the inhibition from AMIGO2 knockdown. Bioinformatics analysis based on RNA sequencing indicated that the interaction between AMIGO2 and *CAPN2* might be involved in multiple signaling pathways.

Conclusions: Our work suggests that AMIGO2 promotes the proliferation and migration of HPSCC by interacting with *CAPN2*, implying that AMIGO2 can be therapeutically targeted to treat HPSCC.

Introduction

Hypopharyngeal squamous cell carcinoma (HPSCC) is one of the most common malignant tumors in the head and neck area, and it caused at least 38,599 deaths worldwide in 2020[1]. Due to the lack of specific signs and early symptoms, most HPSCC patients are diagnosed at an advanced stage[2]. Although treatments including surgery, radiotherapy, chemotherapy, and immunotherapy show promises in the management of Head-Neck Squamous Cell Carcinoma (HNSC), the prognosis of HPSCC patients remains extremely poor[2–4]. Insights into the tumorigenic mechanisms underlying HPSCC are therefore of great importance in achieving early diagnosis and in finding potential therapeutic targets.

Amphoterin-induced gene and open reading frame 2 (*AMIGO2*) is a type I transmembrane protein that contains a signal sequence for secretion[5]. As a member of three structurally homologous type I transmembrane proteins (the *AMIGO* family), *AMIGO2* was firstly discovered in neurons treated with the neurite-promoting protein amphoterin and proposed as a cellular adhesion molecule involved in neurite formation[5]. *AMIGO2* had been recently shown to play a vital role in many types of cancers—including colorectal, gastric, and ovarian cancers, as well as melanoma[6–9]. However, the information about the relationship between *AMIGO2* and HPSCC remains limited.

In the present study, we first investigated the differential expression and prognostic value of *AMIGO2* in HNSC and other cancer types. By using short hairpin RNAs (shRNAs) to stably knock down *AMIGO2* expression *in vivo* and *in vitro*, we found that *AMIGO2* promoted the proliferation and migration of HPSCC. Liquid chromatography-tandem mass spectrometry (LC-MS/MS) and co-immunoprecipitation (Co-IP) revealed an interaction between *AMIGO2* and *CAPN2* (Calpain2), and overexpression of the latter partially reversed the inhibitory effect caused by *AMIGO2* knockdown. Gene Ontology (GO) and Kyoto Encyclopedia of Genes and Genomes (KEGG) analysis based on RNA sequencing further suggested that the oncogenic roles of *AMIGO2* and *CAPN2* might be involved in multiple signaling pathways.

Materials And Methods

Cell culture

The human HPSCC cell line FaDu, the human laryngeal cancer cell line HEp-2 and HEK293T cell line were purchased from Shanghai GeneChem Co., Ltd. Cells were maintained in Minimum Essential Medium (MEM, Thermo) supplemented with 10% fetal bovine serum (FBS, Gibco) at 37°C in a humidified atmosphere of 5% CO_2 in compressed air.

Western blot

Proteins were extracted with a lysis buffer, quantified using a bicinchoninic acid (BCA) protein quantification kit (KeyGen Biotech), and lysates were separated using 10% SDS-PAGE and transferred onto a PVDF membrane (Millipore). The membrane was then incubated with specific primary antibodies (listed in Table 1) followed by the appropriate secondary antibodies. The protein bands on the membranes were visualized using the ECL Western Blotting Substrate Kit (Pierce, Thermo) according to the manufacturer's instructions.

Table 1
Primary antibodies used for western blotting.

Antibody	Company	Cat. #
AMIGO2	Proteintech	14076-1-AP
HDAC2	abcam	ab32117
RHOA	abcam	ab187027
NDRG1	abcam	ab124689
CAPN2	abcam	ab75994
PXN	abcam	ab32084
GAPDH	Santa-Cruz	sc-2004
β-actin	Santa Cruz	sc-69879
Flag	Sigma	F1804

Real-time quantitative PCR (qPCR)

Total RNA was extracted from cells using Trizol reagent (Invitrogen) according to the manufacturer's instructions. RNA reverse-transcription to cDNA was performed with M-MLV reverse transcriptase (Promega), and qPCR amplification was performed with a SYBR Premix Ex Taq II kit (Takara). Relative expressions of target genes were calculated using the $2^{-\triangle\triangle Ct}$ method and GAPDH was considered as a reference gene for normalization. The sequences of the *AMIGO2* primers were F: CCTGGGAACCTTTTCAGACTG and R: GCAAACGATACTGGAATCCACT. The sequences of the GAPDH primers were F: TGACTTCAACAGCGACACCCA, R: CACCCTGTTGCTGTAGCCAAA.

Gene silencing and overexpression

Knockdown of *AMIGO2* was performed with shRNAs. The sh*AMIGO2* lentivirus and scrambled shRNA control were purchased from Shanghai GeneChem Co., Ltd. The targeting RNAi sequences of two different shRNAs and scrambled control were as follows: sh*AMIGO2*-1, 5'-AATTTCACTGTAAGCAGAT-3'; sh*AMIGO2*-2, 5'-CTTGACTTATCGTCCAATA-3'; and shCtrl, 5'-TTCTCCGAACGTGTCACGT-3'. The shRNA-expressing recombinant plasmids (hU6-MCS-CMV-EGFP, GV115, GeneChem; 20 μg) along with two helper plasmids, pHelper 1.0 (GeneChem; 15 μg) and 2.0 (GeneChem; 10 μg) were transfected into 293T cells (American Type Culture Collection) using a transfection reagent (GeneChem). Overexpressions of *AMIGO2* and *CAPN2* were mediated by lentiviruses designed and constructed by Shanghai GeneChem Co., Ltd. The recombinant lentivirus was produced by transfecting into HEK293T cells as described above. The generated lentiviruses were filtered, enriched, and added to cultured FaDu cells. Puromycin was then added to select the stable cells, and the efficiency of target-gene knockdown and/or overexpression was verified by western blotting and qPCR.

Proliferation assays

Cell proliferation was assessed using Celigo cell-counting and MTT assay. Briefly, following lentiviral transfection, FaDu cells were seeded onto 96-well plates at a density of 800 cells per well and grown for up to 5 days. We observed and recorded the green-fluorescence emission each day using the Celigo Cell Counting system (Nexcelom) according to the manufacturer's instructions. For the MTT assay, FaDu cells were cultured in 96-well culture plates at a density of 2×10^3 cells per well overnight. We added MTT solution (Genview, Cat# JT343) at the desired timepoints, allowed the cells to remain in culture for 4 h, and then evaluated them at 490 nm on a microplate reader (Tecan infinite, Cat# M2009PR) according to the manufacturer's protocol.

Apoptosis assay using flow cytometry

Analysis of apoptosis based on fluorescence-activated cell sorting (FACS) was conducted with the Annexin V-APC Apoptosis Detection Kit (eBioscience, Cat# 88-8007) according to the manufacturer's instruction. In brief, 72 h after infection the adherent and nonadherent cells were collected, washed once in 1× binding buffer, and resuspended in 1× staining buffer at 5×10^6 cells/ml. We then incubated 200 µl of cells with 10 µl of annexin V-APC at room temperature for 15 min in the dark. Annexin V-stained cells were then assessed using a FACScan flow cytometer (Becton–Dickinson, FACSCalibur) according to the manufacturer's protocol.

Migration assays

The migratory ability of FaDu cells was observed by wound-healing assay 3 days after transfection using an Oris™ plate (Platypus Technologies) and a Celigo Image Cytometer (Nexcelom). Briefly, the cells were collected and seeded onto 96-well plates at the appropriate concentration ($3–5 \times 10^4$ per well), and the plates containing Oris™ Pro Biocompatible Gel were incubated in a humidified chamber (at 37°C in 5% CO_2/air) for 24 h. The plates were taken from the incubator the next day, and the inserts were removed from the wells. After the wells were washed with serum-free medium, low-serum medium (1% FBS) was added to the wells, and the cells were examined using Celigo (Nexcelom) to monitor the progression of migration at 0 h, 24 h, and 48 h.

Cell migratory capability was also determined using 24-well cell culture Transwell chambers (Corning, Cat# 3422). FaDu cells (1×10^5/ well) were suspended in 100 µl of serum-free medium and plated into the upper chambers, and 600 µl of medium containing 30% FBS was placed into the lower chambers. After 48 or 60 h, the cells under the bottom membrane were stained with crystal violet. The migrating cells in nine randomly selected fields at a magnification of ×200 were imaged using digital microscopy and counted. All assays were performed in triplicate.

Xenograft mouse model

Four-week-old BALB/c female nude mice (Beijing Vital River Laboratory Animal Technology Co., Ltd.; certificate no. SCXK[Hu]2017-0011) were reared in a specific-pathogen-free (SPF) room. A total of 5×10^6

cells were injected into the axilla subcutaneously, and xenograft tumor sizes were measured two or three times per week. After three weeks, all nude mice were sacrificed, and xenograft tumors were removed, photographed, and weighed. Tumor volume was calculated according to the following formula: $V = \pi/6 \times L \times W^2$, where L and W represented the largest and smallest diameters of the tumor.

Co-IP and LC–MS/MS

FaDu cells that stably expressed 3xFlag-*AMIGO2* and negative controls were lysed separately with immunoprecipitation lysis buffer (Beyotime). The cell lysates were incubated overnight with an anti-FLAG agarose affinity gel (Sigma, Cat# A2220). The immune complexes were then eluted with low-pH buffer and separated by SDS-PAGE, followed by Coomassie blue staining. All candidate protein bands were excised from the gels, trypsin digested in-gel, and subjected to nano LC–MS/MS on a Q Exactive mass spectrometer (Thermo); the results were analyzed by Mascot as previously described[10]. Based on LC–MS/MS results and subsequent bioinformatics analysis, HDAC2, RHOA, NDRG1, *CAPN2*, and PXN were selected for further co-IP validation. As described above, the immunocomplexes were then detected by western immunoblotting with specific antibodies (listed in Table 1).

RNA sequencing

RNA preparation, library construction, and sequencing were performed on the Illumina Novaseq platform at Shanghai GeneChem Co., Ltd., as previously reported[11].

Bioinformatics analysis

The Cancer Genome Atlas (TCGA, https://cancergenome.nih.gov/) is a prestigious cancer genomics project funded by the National Cancer Institute, USA, and characterizes more than 20,000 primary cancer and matched normal-tissue samples from various cancer types[12]. The differential expression of *AMIGO2* in various cancers from TCGA was visualized in the “Gene_DE” module of Tumor Immune Estimation Resource 2 (TIMER2, http://timer.cistrome.org/), an online tool for systematic analysis of immune infiltrates across diverse cancer types[13]. PrognoScan (http://gibk21.bse.kyutech.ac.jp/PrognoScan) is a publicly accessible and powerful platform for evaluating the association between a gene and clinical outcome in cancers[14]. Survival analysis of HNSC with respect to *AMIGO2* expression was conducted on PrognoScan (dataset: GSE2837[15]). We determined the correlation between *AMIGO2* expression and survival in head and neck cancer using the Kaplan-Meier plotter (https://kmplot.com/analysis/), a powerful website used to assess the effect of 54,000 genes on survival in 21 types of cancer. The Ingenuity Pathway Analysis system (IPA; Qiagen) was used to analyze the results from LC-MS/MS coupled with Co-IP to ascertain potential *AMIGO2*-binding proteins.

We also executed differential expression analysis using the DESeq2 R package (1.16.1). The resulting P-values were adjusted using the Benjamini and Hochberg approach for controlling the false-discovery rate, and genes with a |log2FoldChange| >0.0 and an adjusted P-value < 0.05 as determined by DESeq2 were assigned as differentially expressed. GO analysis of differentially expressed genes was implemented with

the clusterProfiler R package, in which gene-length bias was corrected. GO terms with corrected P values less than 0.01 were considered significantly enriched by differentially expressed genes. KEGG is a database resource for understanding high-level functions and utilities of biologic systems such as the cell, the organism, and the ecosystem, and encompasses molecular-level information and particularly large-scale molecular datasets generated by genome sequencing and other high-throughput experimental technologies (http://www.genome.jp/kegg/). We used the clusterProfiler R package to test the statistical enrichment of differentially expressed genes in KEGG pathways (P-value < 0.01).

Statistical analysis

We analyzed data using GraphPad Prism (version 9.1.1, macOS, United States). The results are expressed as means ± the standard deviation (SD) of at least three independent experiments. Differences were analyzed using Student's *t* test, and pairwise multiple comparisons were analyzed by using one-way analysis of variance (ANOVA). $P < 0.05$ was considered statistically significant (* $p < 0.05$; ** $p < 0.01$; *** $p < 0.001$).

Results

AMIGO2 is highly expressed in HNSC and correlates with poor prognosis

We investigated the expression level of *AMIGO2* in different cancers based on RNA sequencing data in TCGA using TIMER2. The differential expression patterns of *AMIGO2* in tumor and adjacent normal tissues are showed in Fig. 1A. The expression level of *AMIGO2* was significantly higher in head and neck cancer and six other cancer types relative to normal tissue. Furthermore, survival analysis based on dataset GSE2837 showed that the *AMIGO2* expression level was significantly correlated with poor prognosis in HNSC (HR = 1.41, 95% CI 1.06–1.86, Fig. 1B). By using the Kaplan-Meier plotter (which is mainly based on Affymetrix microarray information from TCGA), we further assessed the relationship between *AMIGO2* and patient prognosis in head and neck cancer. Our results showed that a high expression of *AMIGO2* was significantly correlated with poor overall survival (OS) and relapse-free survival (RFS) outcomes (OS: HR = 1.42, 95% CI 1.08–1.86, log-rank P = 0.011, Fig. 1C; RFS: HR = 2.83, 95% CI 1.14–7, log-rank P = 0.019, respectively, Fig. 1D).

AMIGO2 knockdown inhibits HPSCC cell proliferation and migration in vitro

To investigate the biologic role of *AMIGO2* in HPSCC, we constructed two independent shRNAs to stably suppresse *AMIGO2* expression in the HPSCC cell line FaDu. *AMIGO2* mRNA abundance in FaDu was first validated by qPCR and compared with the laryngeal cancer cell line HEp-2 (**Additional file 1: Figure S1A**), followed by lentiviral transfection. The results of qPCR and western blot then confirmed that the two *AMIGO2* shRNAs remarkably reduced *AMIGO2* expression in FaDu cells at both the mRNA and protein levels (**Additional file 1: Figure S1B, S1C**). Cell-counting and viability assays following transfection of

shRNAs revealed that knockdown of *AMIGO2* significantly inhibited the proliferative capability of FaDu cells (Fig. 2A-2E). On the other hand, analysis of cellular apoptosis based on FACS showed that *AMIGO2* knockdown could effectively promote the apoptosis of FaDu cells (Fig. 2F, 2G). Wound healing assay confirmed that *AMIGO2* knockdown markedly reduced the migratory ability of FaDu cells (Fig. 2H–2I).And the transwell migration assay showed similar results (Fig. 2J-2L**)**.

AMIGO2 knockdown abrogated the proliferation of HPSCC in vivo

To identify the effect of knocking down *AMIGO2* on HPSCC growth *in vivo*, we established a cell-line-derived tumor xenograft model. A total of $5x10^6$ FaDu cells that were transfected with sh-*AMIGO2* (KD) or sh-NC (NC) were inoculated into the right axilla of nude mice, followed by consecutive tumor-growth assessments (Fig. 3A). After three weeks, the mice were sacrificed, and the xenograft tumors were then enucleated and analyzed. However, the xenograft tumor failed to grow in eight mice of KD group after inoculation (Fig. 3B). The tumor volume and weight in KD group were significantly smaller than those in NC group (Fig. 3C, 3D), indicating that *AMIGO2* knockdown greatly abrogated the tumor growth. Collectively, these results suggested that *AMIGO2* might play a pro-tumor role in the proliferation and migration of HPSCC cells.

AMIGO2 interacts with CAPN2 in HPSCC

To further explore the molecular mechanism underlying the action of *AMIGO2* in HPSCC, we designed a 3×FLAG-*AMIGO2* overexpression lentivirus to transfect into FaDu cells (OE), with FaDu cells transfected with lenti-Control virus as a negative control (NC). Western blot results of puromycin-selected stable cells confirmed that the FLAG-tag fusion target protein (*AMIGO2*) was successfully overexpressed in the OE group (**Additional file 1: Figure S1D**). We performed preliminary Co-IP experiments to confirm that *AMIGO2* was overexpressed in target cells, and FLAG-tag was exposed and detected by anti-FLAG antibody as we expected (Fig. 4A). Protein complex samples (Fig. 4B) purified from NC and OE via preliminary Co-IP experiments were then analyzed by LC-MS/MS. Bioinformatics analysis based on the LC-MS/MS results revealed that *AMIGO2* exhibited potential protein-protein interactions with *HDAC2*, *RHOA*, *NDRG1*, *CAPN2*, and *PXN* (Fig. 4C). Co-IP experiments were then performed on FaDu cells using anti-FLAG antibody and antibodies specific to *HDAC2*, *RHOA*, *NDRG1*, *CAPN2*, and *PXN*, and the results revealed that *AMIGO2* physiologically bound with *CAPN2* in FaDu cell context (Fig. 4D).

Overexpression of CAPN2 attenuates the inhibition of cellular proliferation and migration by AMIGO2 knockdown

To evaluate the role of *CAPN2* in the relationship between *AMIGO2* and HPSCC, plasmids containing a *CAPN2*-expression cassette were transfected into FaDu cells manifesting knockdown of *AMIGO2*. Cell-counting assay revealed that overexpression of *CAPN2* could significantly attenuate the inhibition of *AMIGO2* knockdown on proliferation (Fig. 5A, 5B). Cell viability assay also further confirmed that overexpressing *CAPN2* could neutralize the inhibition by knockdown of *AMIGO2* on proliferation of

HPSCC cells (Fig. 5C, 5D). The transwell migration assay results subsequently indicated that while knockdown of *AMIGO2* decreased the migratory ability of HPSCC cells as anticipated, overexpression of *CAPN2* markedly promoted the migration of *AMIGO2*-silenced FaDu cells (Fig. 5E-5G). These results collectively revealed that overexpression of *CAPN2* attenuated the inhibitory effect of *AMIGO2* silencing on cellular proliferation and migration of HPSCC cells.

Pathway enrichment analysis of AMIGO2 and CAPN2

To determine how *AMIGO2* and *CAPN2* affected the progression of HPSCC, RNA-seq analysis was performed on three groups of FaDu cells, i.e., *AMIGO2* knockdown (KD_NC), *AMIGO2* knockdown combined with *CAPN2*-overexpression (KD_OE), and normal controls (NC_NC). We identified 2294 up-regulated and 2375 down-regulated genes in the comparison between the KD_NC and NC_NC groups (Fig. 6A, **Additional file 3: Table S1**); 3200 up-regulated and 3867 down-regulated genes in the comparison between the KD_OE and KD_NC groups (Fig. 6B, **Additional file 4: Table S2**); and 4367 up-regulated and 4923 down-regulated genes between KD_OE and NC_NC groups (Fig. 6C, **Additional file 5: Table S3**). Hierarchical clustering and an expression heatmap of all differentially expressed genes (DEGs) are showed in Fig. 6D.

A set of 817 overlapping DEGs were found between up-regulated genes upon *AMIGO2* knockdown (KD_NC vs. NC_NC) and down-regulated genes upon *CAPN2*-overexpression (KD_OE vs. KD_NC). Another set of 546 overlapping DEGs was found between down-regulated genes upon *AMIGO2* knockdown (KD_NC vs. NC_NC) and up-regulated genes upon *CAPN2*-overexpression (KD_OE vs. KD_NC). Based on a total 1363 genes from these two sets of overlapping DEGs (Fig. 6E), we subsequently conducted pathway enrichment analysis. GO analysis results showed that these 1363 DEGs were significantly enriched in biological processes (BP, Fig. 6F), molecular functions (MF, Fig. 6G), and cell components (CC, Fig. 6H)—including extracellular matrix organization (BP), extracellular structure organization (BP), regulation of cell-cell adhesion (BP), protease binding (MF), cell-substrate junction (CC), cell-cell junction (CC), and focal adhesion (CC). KEGG analysis results indicated that multiple pathways were significantly enriched—including human papillomavirus (HPV) infection and PI3K-Akt signaling pathway (Fig. 6I).

Discussion

HPSCC is a less prevalent yet aggressive malignancy in the head and neck region. Absence of symptoms in its early phase and a high rate of regional and systemic metastases make HPSCC the most lethal of head and neck cancers[2, 4]. A large proportion of HPSCC patients lack specific early symptoms or pathologic signs in part because of the unique anatomy of the hypopharynx, and, in addition, laryngoscopy is not routine in most countries. Consequently, early detection of HPSCC remains challenging, and it was reported that more than 75% of patients were already in stage III or IV when initially diagnosed[16]. HPSCC patients at advanced stages have limited treatment options and their clinical outcomes are far from satisfactory, although the overall 5-year survival rate has increased from 37.5–41.3%[4]. Elucidation of the molecular events that contribute to cancer cell proliferation and

migration is thus of critical importance in achieving early diagnosis and finding appropriate therapeutic targets.

As a member of the homologous *AMIGO* family, *AMIGO2* was first found by ordered differential display in neuronal tissues treated with neurite-promoting protein, and it was regarded as a novel cell-adhesion molecule that contributes to neuronal formation[5]. Also known as Alivin 1, *AMIGO2* was discovered by another research group that reported its promotion of the neuronal activity-dependent survival of cerebellar granule neurons[17]. An etiologic role for *AMIGO2* (also known as DEGA) in gastric adenocarcinoma was subsequently reported[18]. Furthermore, emerging data suggested a detrimental action of *AMIGO2* in multiple cancer types, including melanoma[6], liver[19], gastric[8], colorectal[7], and ovarian cancer[9]. Based on these previous reports, we hypothesized an oncogenic role for *AMIGO2* in HPSCC.

In the current study, we found *AMIGO2* to be up-regulated in HNSC tumors when compared to adjacent normal tissues based on TCGA data, and high expression levels of *AMIGO2* were correlated with a poor prognosis in HNSC. We further confirmed that *AMIGO2* exhibited a higher mRNA abundance in the HPSCC cell line FaDu relative to the laryngeal cancer cell line HEp-2. *AMIGO2* silencing by shRNAs markedly suppressed cellular proliferation and migration while promoting the apoptosis of FaDu cells *in vitro*, and knockdown of *AMIGO2 in vivo* also significantly reduced xenograft tumor growth, as expected. Similar to our results, *AMIGO2* was reported to be differentially expressed in nearly half of the gastric adenocarcinoma patients, and its knockdown led to nearly complete abrogation of tumorigenicity[18]. Additionally, *AMIGO2* was identified as the most highly differentially expressed gene in the process of in-vivo selection of a metastatic ovarian cancer cell line[9]. Collectively, our results indicated that *AMIGO2* promoted tumor proliferation and migration in HPSCC.

Based on LC-MS/MS and bioinformatics analysis results, we uncovered five proteins that potentially interact with *AMIGO2*. Co-IP experiments confirmed that in the FaDu cellular context, *AMIGO2* elicited protein-protein interactions with *CAPN2*. *AMIGO2*-silenced inhibition of cellular proliferation might thus be partially attenuated by the overexpression of *CAPN2*. Furthermore, *CAPN2* overexpression notably counteracted the inhibition on migration by *AMIGO2* silencing. These results suggested that *CAPN2* is a key molecule responsible for the biologic effects of *AMIGO2* in HPSCC. *CAPN2* encodes a distinct catalytic subunit of calpain-2, a calcium-dependent intracellular thiol protease that is ubiquitously expressed in tissues[20]. Investigators had previously demonstrated an oncogenic role for calpain-2 in numerous types of cancers, including colorectal[21], mammary[22], and hepatocellular cancers[23]—as well as acute myelogenous leukemia[24]. For example, in breast cancer calpain-2 promotes tumor cell proliferation and migration both *in vitro* and *in vivo* via regulation by Akt[22]. Moreover, calpain-2 serves as a diagnostic marker in non-small cell lung cancer, and as a potential treatment target in colorectal cancer as well as in gefitinib-resistant lung adenocarcinoma[25–27].

Upon investigation of the synergistic effects of *AMIGO2* and *CAPN2* (calpain-2) in HPSCC, we found that multiple signaling pathways were significantly enriched in KEGG analysis, including HPV infection and

PI3K-Akt signaling pathway. HPV infection has been known as an aetiological risk factor for HNSCC for decades[28]. HPV-positive HNSC shows a unique tumorigenic biology and exhibits distinct differences from HPV-negative HNSC in many aspects, including gene expression and immune profiles[29]. While HPV positivity were relevantly less common in HPSCC, it was associated with an improved survival, indicating a potientially different clinical management strategy[30, 31]. Although HPV infection pathway was markedly enriched upon regulation of *AMIGO2* and *CAPN2*, it is still unknown whether these genes (proteins) could facilitate or hinder HPV infection in hypopharynx, and more experiments are needed in future to answer this question. For another, PI3K-Akt signaling is a well-documented pathway and regarded as one of the most frequently dysregulated pathways in human cancers[32–35]. In brief, phosphoinositide 3-kinase (PI3K) activated by multiple stimuli phosphorylates phosphatidylinositol-4,5-bisphosphate (PIP2) to generate phosphatidylinositol-3,4,5-trisphosphate (PIP3)[36]. PIP3 then recruits phosphoinositide-dependent protein kinase-1 (PDK1) to the plasma membrane, resulting in the activation of Akt by its phosphorylation by PDK1[36, 37]. Notably, the C-terminal region of *AMIGO2* can directly bind to PDK1, regulate the membrane localization of PDK1, and subsequently facilitate Akt activation[38]. Furthermore, *CAPN2* has been reported to mediate the degradation of phosphatase and tensin homolog (PTEN), a protein that dephosphorylates PIP3 to generate PIP2[39]. And degradation of PTEN can then cause accumulation of PIP3, resulting in prolonged activation of the PI3K-Akt pathway[36, 37]. However, in the context of HPSCC, the participation of *AMIGO2* or *CAPN2* in PI3K-Akt signaling pathway still remains unknown and awaits further experiments to validate.

Taken together, our results showed that *AMIGO2* interacts with *CAPN2* and promotes tumor proliferation and migration in HPSCC. Our work thus provided a potential novel molecular mechanism underlying the oncogenesis of HPSCC and supports *AMIGO2* as a potential marker for the diagnosis and therapeutic intervention in HPSCC.

Declarations

Acknowledgement

None.

Funding

This work was funded by the grant to Xiaofeng Jin and Jian Wang from the Strategic Priority Research Program of the Chinese Academy of Sciences (Grant No. XDA1601040201).

Competing Interest

The authors have no conflicts of interest to declare.

Availability of data and materials

The datasets generated and/or analysed during the current study can be found in supplementary files and be obtained from Gene Expression Omnibus (GEO) with an accession number of GSE200657 (https://www.ncbi.nlm.nih.gov/geo/query/acc.cgi?acc=GSE200657).

Authors' contributions

WG, YN, XJ and JW designed the study. WG and YN conducted most of the experiments. HH and DY participated in the overall study design and the revision of the final manuscript. WG performed the data analysis and wrote the draft manuscript. All authors contributed to the article and approved the submitted version.

All experimental animal procedures were performed in accordance with institutional guidelines for the care and use of laboratory animals and the study is reported in accordance with ARRIVE guidelines. The protocols were approved by the Institutional Animal Ethics Committee of Peking Union Medical College Hospital (Permission No. XHDW-2019-037).

Patient consent for publication

Not applicable.

References

1. Sung H, Ferlay J, Siegel RL, Laversanne M, Soerjomataram I, Jemal A, et al. Global Cancer Statistics 2020: GLOBOCAN Estimates of Incidence and Mortality Worldwide for 36 Cancers in 185 Countries. CA Cancer J Clin. 2021;71:209–49.
2. Chan JY, Wei WI. Current management strategy of hypopharyngeal carcinoma. Auris Nasus Larynx. 2013;40:2–6.
3. Carlisle JW, Steuer CE, Owonikoko TK, Saba NF. An update on the immune landscape in lung and head and neck cancers. CA Cancer J Clin. 2020;70:505–17.
4. Newman JR, Connolly TM, Illing EA, Kilgore ML, Locher JL, Carroll WR. Survival trends in hypopharyngeal cancer: a population-based review. Laryngoscope. 2015;125:624–9.
5. Kuja-Panula J, Kiiltomäki M, Yamashiro T, Rouhiainen A, Rauvala H. AMIGO, a transmembrane protein implicated in axon tract development, defines a novel protein family with leucine-rich repeats. J Cell Biol. 2003;160:963–73.
6. Fontanals-Cirera B, Hasson D, Vardabasso C, Di Micco R, Agrawal P, Chowdhury A, et al. Harnessing BET Inhibitor Sensitivity Reveals AMIGO2 as a Melanoma Survival Gene. Mol Cell. 2017;68:731–744.e9.
7. Tanio A, Saito H, Amisaki M, Hara K, Sugezawa K, Uejima C, et al. AMIGO2 as a novel indicator of liver metastasis in patients with colorectal cancer. Oncol Lett. 2021;21:278.
8. Nakamura S, Kanda M, Shimizu D, Tanaka C, Inokawa Y, Hattori N, et al. AMIGO2 Expression as a Potential Prognostic Biomarker for Gastric Cancer. Anticancer Res. 2020;40:6713–21.

9. Liu Y, Yang J, Shi Z, Tan X, Jin N, O'Brien C, et al. In vivo selection of highly metastatic human ovarian cancer sublines reveals role for AMIGO2 in intra-peritoneal metastatic regulation. Cancer Lett. 2021;503:163–73.
10. Scifo E, Szwajda A, Soliymani R, Pezzini F, Bianchi M, Dapkunas A, et al. Proteomic analysis of the palmitoyl protein thioesterase 1 interactome in SH-SY5Y human neuroblastoma cells. J Proteomics. 2015;123:42–53.
11. Chen S, Yang C, Wang Z-W, Hu J-F, Pan J-J, Liao C-Y, et al. CLK1/SRSF5 pathway induces aberrant exon skipping of METTL14 and Cyclin L2 and promotes growth and metastasis of pancreatic cancer. J Hematol OncolJ Hematol Oncol. 2021;14:60.
12. Tomczak K, Czerwińska P, Wiznerowicz M. The Cancer Genome Atlas (TCGA): an immeasurable source of knowledge. Contemp Oncol Poznan Pol. 2015;19:A68-77.
13. Li T, Fu J, Zeng Z, Cohen D, Li J, Chen Q, et al. TIMER2.0 for analysis of tumor-infiltrating immune cells. Nucleic Acids Res. 2020;48:W509–14.
14. Mizuno H, Kitada K, Nakai K, Sarai A. PrognoScan: a new database for meta-analysis of the prognostic value of genes. BMC Med Genomics. 2009;2:18.
15. Chung CH, Parker JS, Ely K, Carter J, Yi Y, Murphy BA, et al. Gene expression profiles identify epithelial-to-mesenchymal transition and activation of nuclear factor-kappaB signaling as characteristics of a high-risk head and neck squamous cell carcinoma. Cancer Res. 2006;66:8210–8.
16. Petersen JF, Timmermans AJ, van Dijk BAC, Overbeek LIH, Smit LA, Hilgers FJM, et al. Trends in treatment, incidence and survival of hypopharynx cancer: a 20-year population-based study in the Netherlands. Eur Arch Otorhinolaryngol. 2018;275:181–9.
17. Ono T, Sekino-Suzuki N, Kikkawa Y, Yonekawa H, Kawashima S. Alivin 1, a Novel Neuronal Activity-Dependent Gene, Inhibits Apoptosis and Promotes Survival of Cerebellar Granule Neurons. J Neurosci. 2003;23:5887–96.
18. Rabenau KE, O'Toole JM, Bassi R, Kotanides H, Witte L, Ludwig DL, et al. DEGA/AMIGO-2, a leucine-rich repeat family member, differentially expressed in human gastric adenocarcinoma: effects on ploidy, chromosomal stability, cell adhesion/migration and tumorigenicity. Oncogene. 2004;23:5056–67.
19. Kanda Y, Osaki M, Onuma K, Sonoda A, Kobayashi M, Hamada J, et al. Amigo2-upregulation in Tumour Cells Facilitates Their Attachment to Liver Endothelial Cells Resulting in Liver Metastases. Sci Rep. 2017;7:43567.
20. Goll DE, Thompson VF, Li H, Wei W, Cong J. The Calpain System. Physiol Rev. 2003;83:731–801.
21. Lakshmikuttyamma A, Selvakumar P, Kanthan R, Kanthan SC, Sharma RK. Overexpression of m-calpain in human colorectal adenocarcinomas. Cancer Epidemiol Biomarkers Prev. 2004;13:1604–9.
22. Ho W, Pikor L, Gao Y, Elliott BE, Greer PA. Calpain 2 Regulates Akt-FoxO-p27Kip1 Protein Signaling Pathway in Mammary Carcinoma *. J Biol Chem. 2012;287:15458–65.
23. Chen B, Tang J, Guo Y-S, Li Y, Chen Z-N, Jiang J-L. Calpains are required for invasive and metastatic potentials of human HCC cells. Cell Biol Int. 2013;37:643–52.

24. Niapour M, Farr C, Minden M, Berger SA. Elevated calpain activity in acute myelogenous leukemia correlates with decreased calpastatin expression. Blood Cancer J. 2012;2:e51–e51.
25. Kwon S-H, Wi T, Park YI, Kim MW, Lee G, Higaki T, et al. Noninvasive Early Detection of Calpain 2-Enriched Non-Small Cell Lung Cancer Using a Human Serum Albumin-Bounded Calpain 2 Nanosensor. Bioconjug Chem. 2020;31:803–12.
26. Marciel MP, Rose AH, Martinez V, Horio DT, Hashimoto AS, Hoffmann FW, et al. Calpain-2 inhibitor treatment preferentially reduces tumor progression for human colon cancer cells expressing highest levels of this enzyme. Cancer Med. 2018;7:175–83.
27. Zhang G, Fang T, Chang M, Li J, Hong Q, Bai C, et al. Calpain 2 knockdown promotes cell apoptosis and restores gefitinib sensitivity through epidermal growth factor receptor/protein kinase B/survivin signaling. Oncol Rep. 2018;40:1937–46.
28. Hennessey PT, Westra WH, Califano JA. Human papillomavirus and head and neck squamous cell carcinoma: recent evidence and clinical implications. J Dent Res. 2009;88:300–6.
29. Johnson DE, Burtness B, Leemans CR, Lui VWY, Bauman JE, Grandis JR. Head and neck squamous cell carcinoma. Nat Rev Dis Primer. 2020;6:92.
30. Wu Q, Wang M, Liu Y, Wang X, Li Y, Hu X, et al. HPV Positive Status Is a Favorable Prognostic Factor in Non-Nasopharyngeal Head and Neck Squamous Cell Carcinoma Patients: A Retrospective Study From the Surveillance, Epidemiology, and End Results Database. Front Oncol. 2021;11:688615.
31. Patel EJ, Oliver JR, Jacobson AS, Li Z, Hu KS, Tam M, et al. Human Papillomavirus in Patients With Hypopharyngeal Squamous Cell Carcinoma. Otolaryngol Neck Surg. 2022;166:109–17.
32. Engelman JA. Targeting PI3K signalling in cancer: opportunities, challenges and limitations. Nat Rev Cancer. 2009;9:550–62.
33. Fruman DA, Rommel C. PI3K and cancer: lessons, challenges and opportunities. Nat Rev Drug Discov. 2014;13:140–56.
34. Yap TA, Bjerke L, Clarke PA, Workman P. Drugging PI3K in cancer: refining targets and therapeutic strategies. Curr Opin Pharmacol. 2015;23:98–107.
35. Janku F, Yap TA, Meric-Bernstam F. Targeting the PI3K pathway in cancer: are we making headway? Nat Rev Clin Oncol. 2018;15:273–91.
36. Hennessy BT, Smith DL, Ram PT, Lu Y, Mills GB. Exploiting the PI3K/AKT Pathway for Cancer Drug Discovery. Nat Rev Drug Discov. 2005;4:988–1004.
37. Vara JÁF, Casado E, de Castro J, Cejas P, Belda-Iniesta C, González-Barón M. PI3K/Akt signalling pathway and cancer. Cancer Treat Rev. 2004;30:193–204.
38. Park H, Lee S, Shrestha P, Kim J, Park JA, Ko Y, et al. AMIGO2, a novel membrane anchor of PDK1, controls cell survival and angiogenesis via Akt activation. J Cell Biol. 2015;211:619–37.
39. Briz V, Hsu Y-T, Li Y, Lee E, Bi X, Baudry M. Calpain-2-Mediated PTEN Degradation Contributes to BDNF-Induced Stimulation of Dendritic Protein Synthesis. J Neurosci. 2013;33:4317–28.

Figures

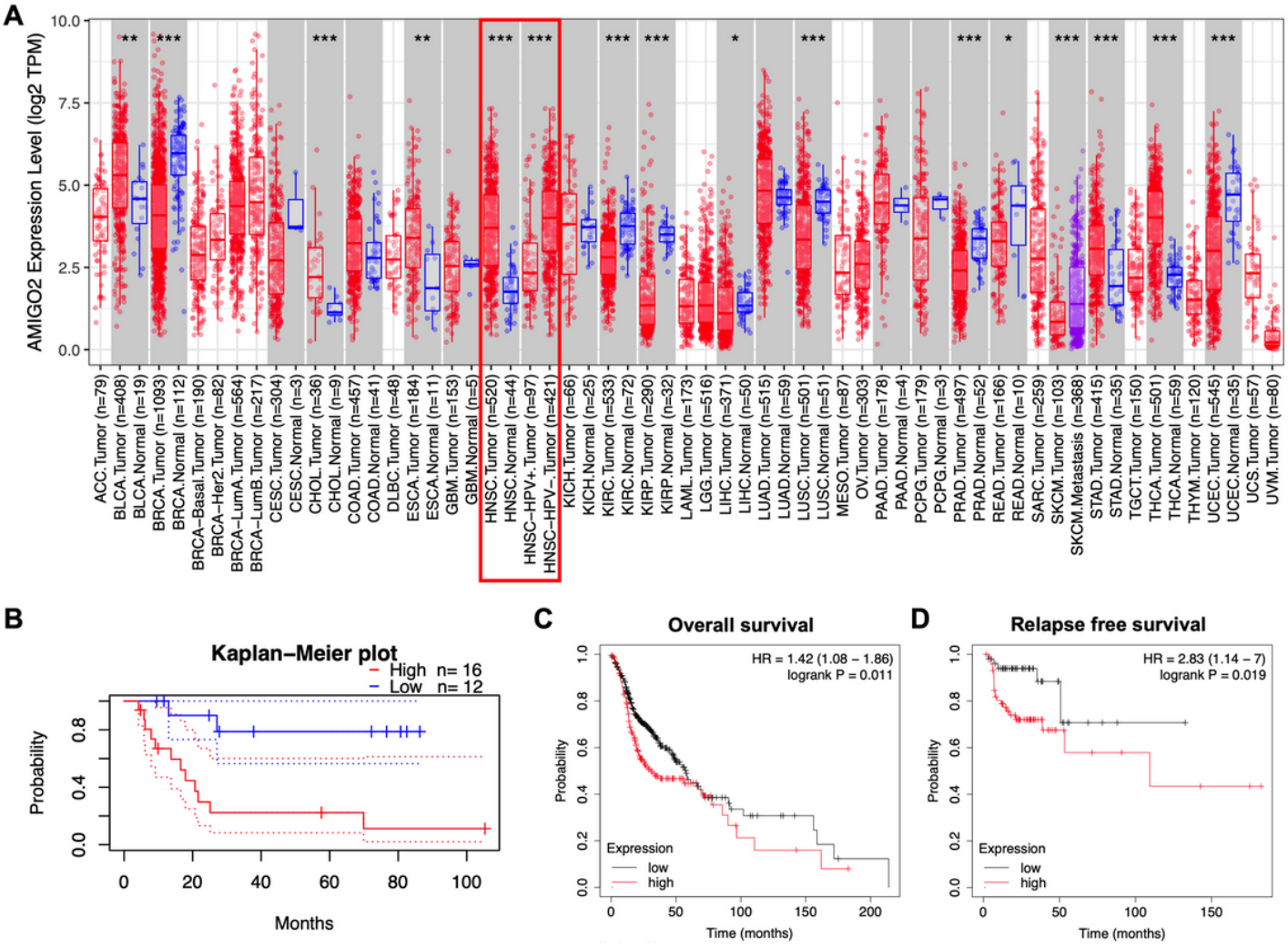

Figure 1

***AMIGO2* expression is up-regulated and correlates with poor outcomes in head and neck cancer (HNSC).** **(A)** Differential expression of *AMIGO2* between tumor and adjacent normal tissues based on TCGA database. *AMIGO2* is up-regulated in HNSC (red-rectangle) and six other cancer types. **(B)** High *AMIGO2* expression level correlates with a poor outcome (relapse free survival) in HNSC patients from dataset GSE2837. **(C)** Overall survival and **(D)** relapse free survival analysis upon *AMIGO2* expression using the Kaplan-Meier plotter website. (* $p < 0.05$; ** $p < 0.01$; *** $p < 0.001$)

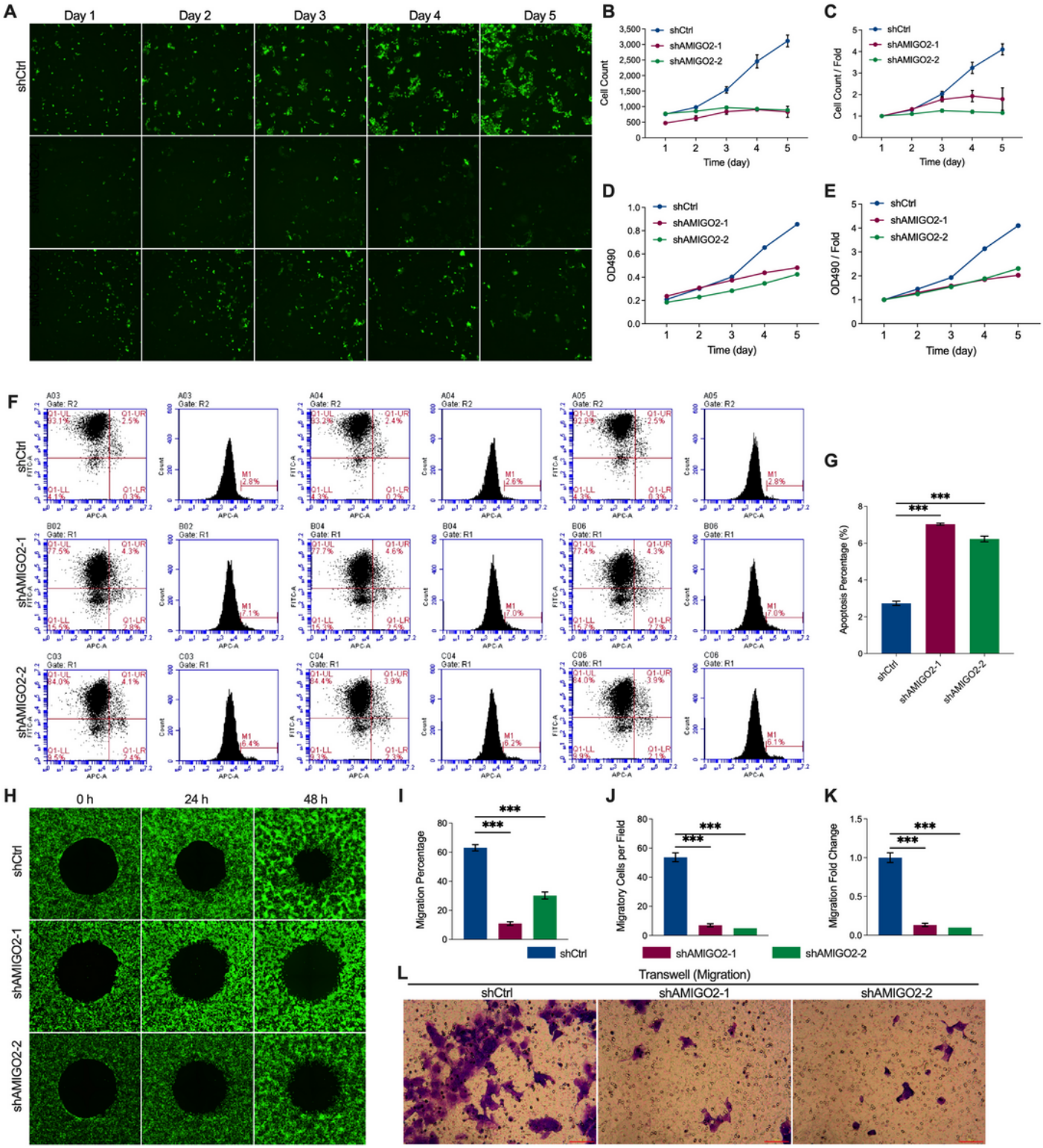

Figure 2

Knockdown of *AMIGO2* attenuates the proliferative and migratory abilities of HPSCC cells *in vitro*. (A-C) Celigo cell-counting in consecutive 5 days showed that *AMIGO2* silencing abrogated the proliferative ability of HPSCC cells. **(D, E)** MTT assay also confirmed impaired proliferative ability of *AMIGO2* knockdown in HPSCC cells. **(F, G)** Apoptotic assay using flow cytometry showed that *AMIGO2* knockdown markedly increased percentage of apoptotic HPSCC cells. **(H, I)** Wound-healing assay results showed

limited migratory ability of HPSCC after knockdown of *AMIGO2*. **(J-L)** Transwell migration assay showed that *AMIGO2* knockdown restricted the migratory capability of HPSCC cells. (Data are presented as means ± SD of at least three independent replicates. * p < 0.05; ** p < 0.01; *** p < 0.001)

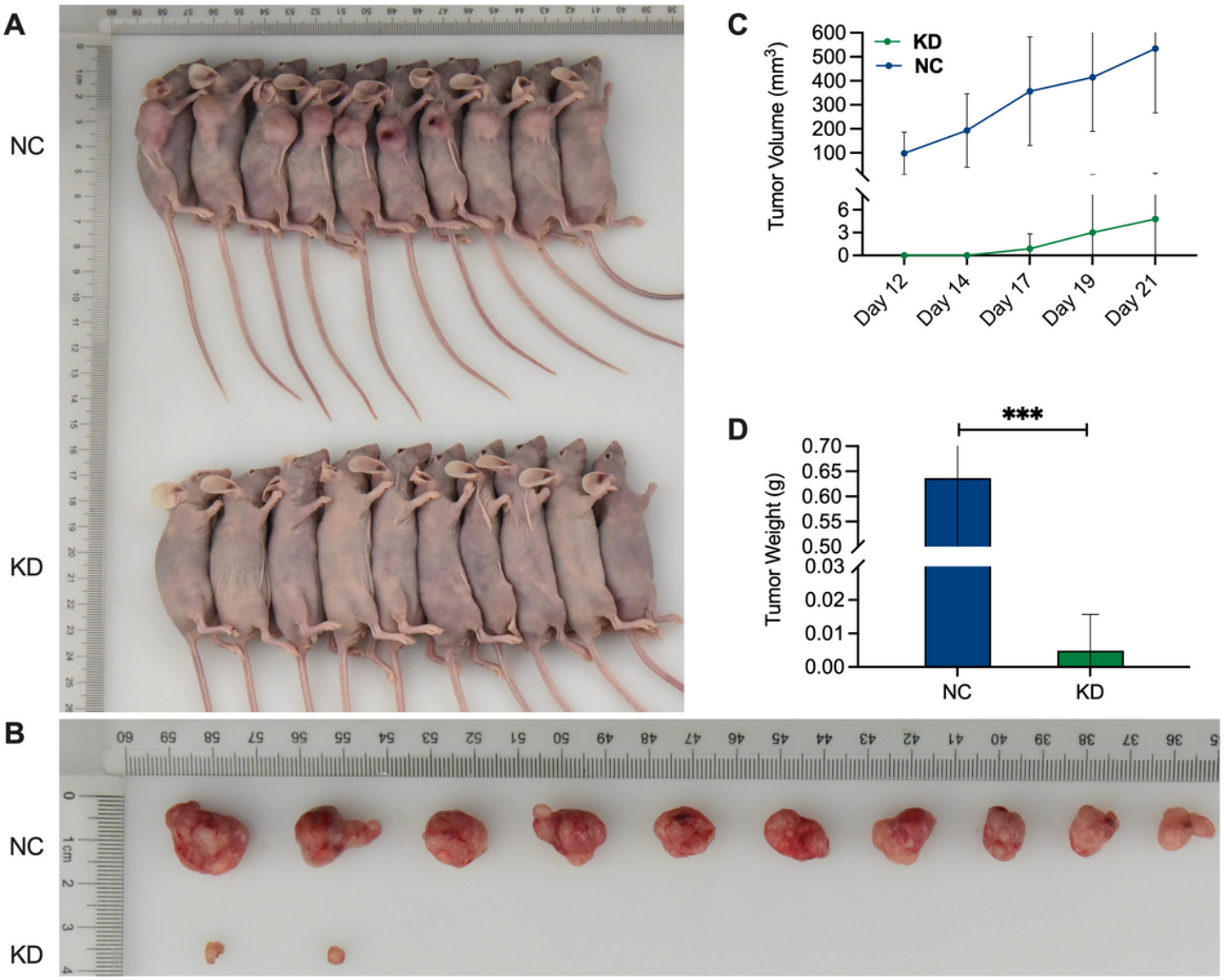

Figure 3

***AMIGO2* knockdown abrogates HPSCC tumor growth *in vivo*. (A)** FaDu cells that were transfected with sh-*AMIGO2* (KD) or sh-NC (NC) were inoculated into the right axilla of nude mice. **(B)** Xenograft tumors were enucleated from 12 nude mice (10 in NC group and 2 in KD group) and measured. **(C)** Tumor volume and **(D)** weight in the KD group were significantly lower than that in the NC group. (Data are presented as means ± SD. * p < 0.05; ** p < 0.01; *** p < 0.001)

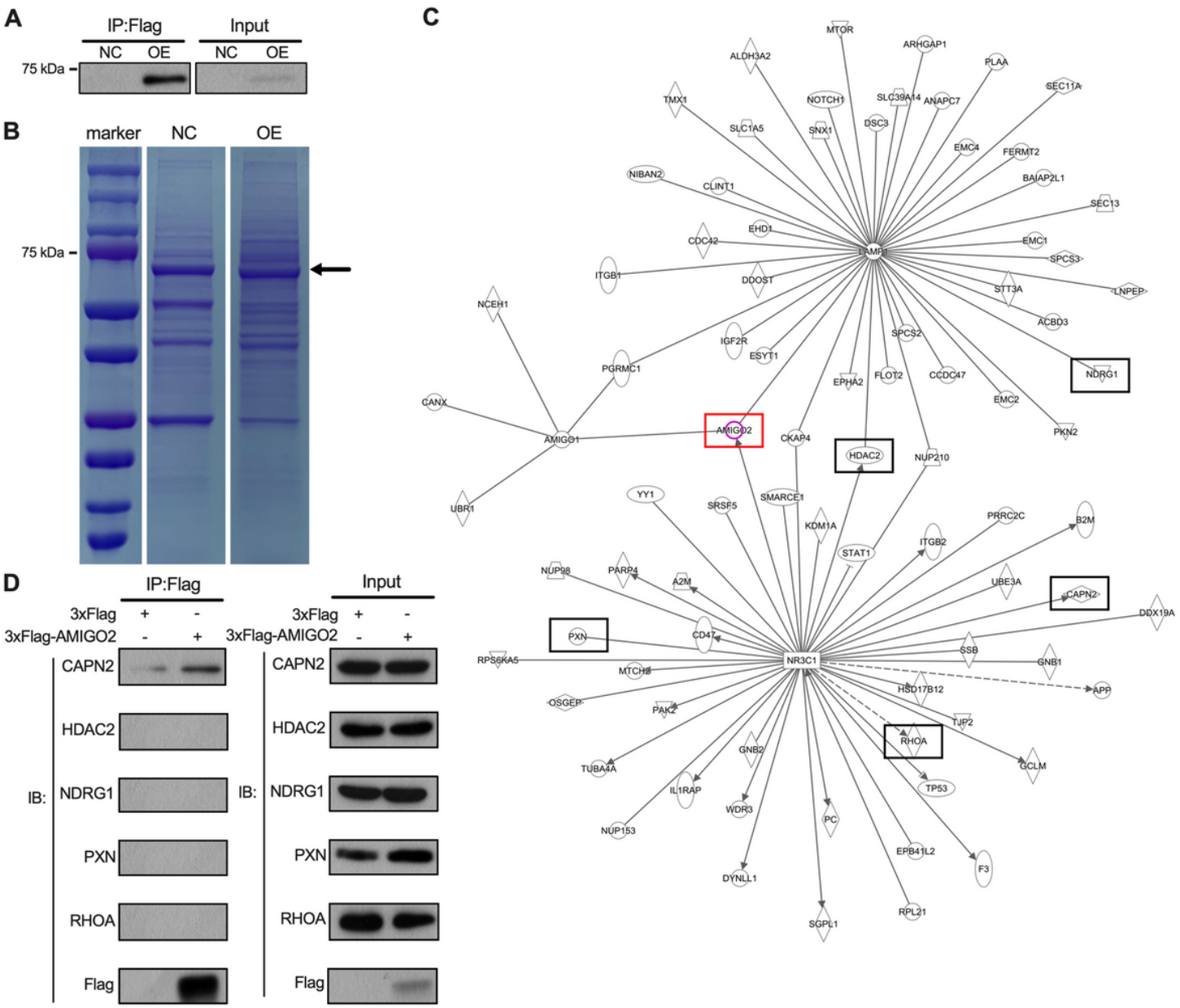

Figure 4

***AMIGO2* interacts with *CAPN2* in a cellular context. (A)** Co-IP preliminary experiment showed that Flag-tag was successfully detected by anti-Flag. **(B)** Purified immune complexes from Co-IP preliminary experiment (anti-Flag) were separated by SDS-PAGE, followed by Coomassie blue staining (black arrow indicates *AMIGO2* protein). Candidate protein bands were then excised for LC-MS/MS analysis. **(C)** IPA analysis based on LC-MS/MS results predicted potential interactions of *AMIGO2* (red rectangle) with HDAC2, RHOA, NDRG1, *CAPN2*, or PXN (black rectangle). **(D)** Co-IP confirmed that *AMIGO2* exhibited a protein-protein interaction with *CAPN2* in a cellular context. (Full-length gels are presented in **Additional file 2**)

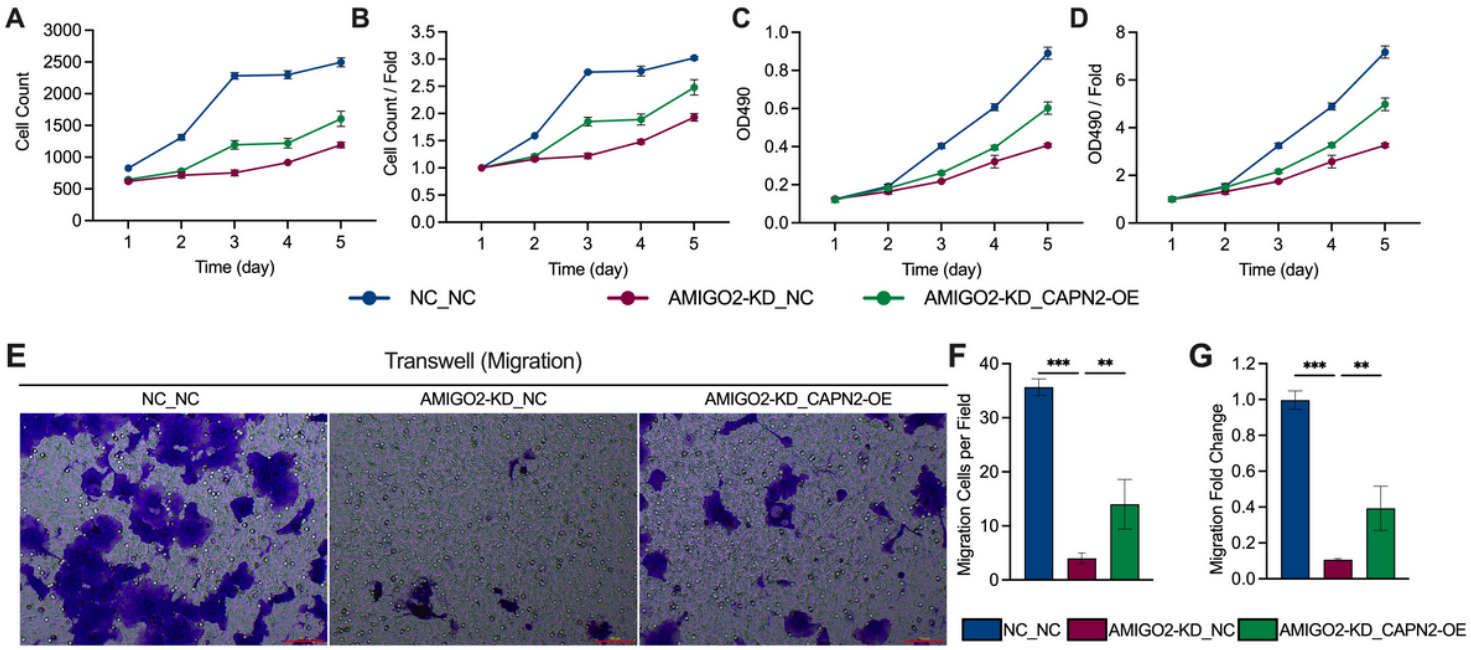

Figure 5

***CAPN2* overexpression attenuated the inhibition of proliferation and migration by *AMIGO2* knockdown.** **(A, B)** Celigo cell-counting results showed that overexpression of *CAPN2* partially reversed the inhibition of proliferation by *AMIGO2* silencing. **(C, D)** MTT assay confirmed that overexpression of *CAPN2* partially reversed the inhibition of proliferation by *AMIGO2* silencing. **(E-G)** Transwell migration assay showed that *CAPN2* overexpression reversed in part the inhibition of HPSCC cell migratory ability by *AMIGO2* knockdown. (Data are presented as means ± SD of three independent replicates. * $p < 0.05$; ** $p < 0.01$; *** $p < 0.001$.)

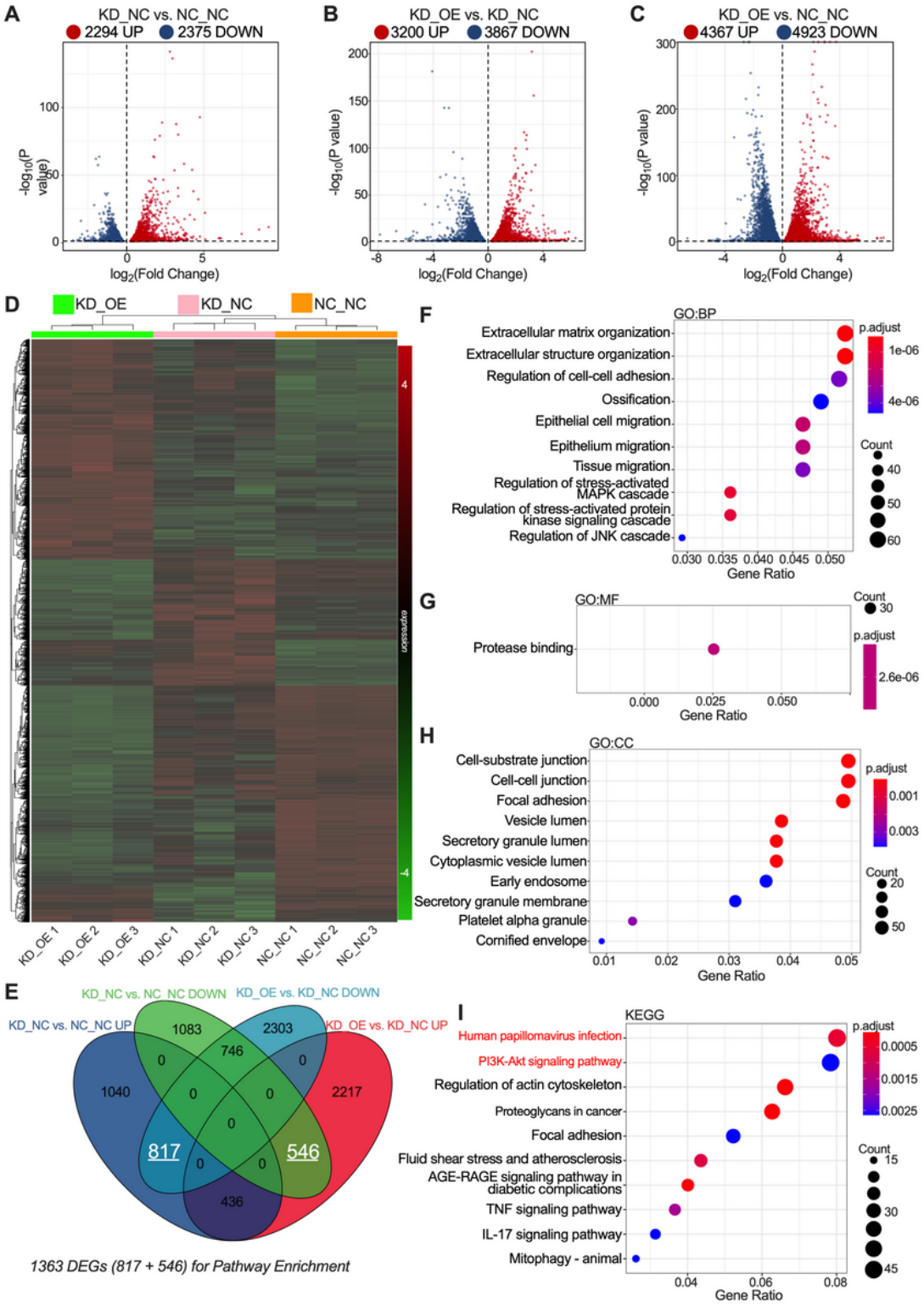

Figure 6

RNA sequencing and pathway-enrichment analysis. Differentially expressed genes (DEGs) were identified in **(A)** KD_NC vs. NC_NC, **(B)** KD_OE vs. KD_NC, and **(C)** KD_OE vs. NC_NC. **(D)** Hierarchical clustering and an expression heatmap of all differentially expressed genes. **(E)** A total of 1363 genes from two sets of overlapping DEGs were used for pathway-enrichment analysis. Gene Ontology (GO)-analysis results showed that 1363 DEGs were significantly enriched in **(F)** extracellular matrix organization, extracellular

structure organization, regulation of cell-cell adhesion, **(G)** protease binding, **(H)** cell-substrate junction, cell-cell junction, and focal adhesion. **(I)** Kyoto Encyclopedia of Genes and Genomes (KEGG) analysis indicated that multiple pathways were significantly enriched, including human papillomavirus infection and PI3K-Akt signaling pathway (red).

Supplementary Files

This is a list of supplementary files associated with this preprint. Click to download.

- Additionalfile1FigureS1.pdf
- Additionalfile2.zip
- Additionalfile3TableS1.xlsx
- Additionalfile4TableS2.xlsx
- Additionalfile5TableS3.xlsx
- Additionalfilesinformation.docx